Chinese Chemical Letters 33 (2022) 2047–2051

Contents lists available at ScienceDirect

Chinese Chemical Letters

journal homepage: www.elsevier.com/locate/cclet

Facile one-pot synthesis of a novel all-carbon stair containing dimerized pentalene core from alkyne

Hui Zhao[a,1], Rakesh Kumar Gupta[a,1], Wei Zhang[b], Jiong Jia[a], Qun Yu[a], Zhiyong Gao[c], Guilin Zhuang[b,*], Dacheng Li[d], Xingpo Wang[a,*], Chen Ho Tung[a], Di Sun[a,*]

[a] Key Laboratory of Colloid and Interface Chemistry, Ministry of Education, School of Chemistry and Chemical Engineering, State Key Laboratory of Crystal Materials, Shandong University, Ji'nan 250100, China
[b] College of Chemical Engineering and Materials Science, Zhejiang University of Technology, Hangzhou 310032, China
[c] School of Chemistry and Chemical Engineering, Collaborative Innovation Center of Henan Province for Green Manufacturing of Fine Chemicals, Key Laboratory of Green Chemical Media and Reactions, Ministry of Education, Henan Normal University, Xinxiang 453007, China
[d] Shandong Provincial Key Laboratory of Chemical Energy Storage and Novel Cell Technology, and School of Chemistry and Chemical Engineering, Liaocheng University, Liaocheng 252000, China

ARTICLE INFO

Article history:
Received 13 August 2021
Revised 13 October 2021
Accepted 15 October 2021
Available online 22 October 2021

Keywords:
One-pot synthesis
Penatlene dimerization
Comproportionation reaction
Crystal structure
Theoretical calculations

ABSTRACT

The construction of all-carbon molecule frameworks remains challenging. Herein, we report a facile and efficient one-pot synthesis of a novel all-carbon stair containing dimerized pentalene core using inexpensive cyclopropyl alkyne catalyzed by *in situ* generated Cu(I) from the comproportionation reaction of Cu(II) salt and Cu powder under mild reaction conditions. The reaction proceeds *via* sequential acetylenic coupling, followed by cyclization and [2 + 2] cycloaddition to directly produce pentalene dimer, which is difficult to access by other established methods. Different mechanistic paths were studied for the pentalene formation using density functional theory, suggesting that the reaction also proceeds through acetylenic coupling followed by cyclization and [2 + 2] cycloaddition. Based on the activation energy barriers, Path 1 has the rate-determining step of 38.63 kcal/mol, which is the most thermodynamically preferred one among the four paths.

During the past few decades, pentalene and its derivatives have attracted much attention of chemists due to their synthetic challenges and antiaromatic characters [1–6]. The chemistry of benzopentalene derivatives has been well explored [7–10]. However, the pentalene dimer or its derivatives are elusive because of multistep syntheses, tedious purification processes, and low synthetic yield. For instance, Neuenschwander *et al.* isolated unsubstituted pentalene dimer by two pathways, firstly oxidative coupling of dilithium pentalenediide dihydropentalene [11] and secondly the removal of hydrogen bromide from 1–bromo-1,2-dihydropentalene resulting in the dimerization of 1–bromo-1,2-dihydropentalene [12]. The dilithium pentalenediide was obtained by the reaction of BuLi and dihydropentalenes, which had to be produced *via* gas-phase pyrolysis of cyclooctatetraene at 400–675 °C [13,14]. Although the synthesis of pentalene by nonpyrolytic methods may also be achieved by the Skattebol rearrangement of a geminal dibromocyclopropane fused cycloheptatriene [15,16], a general method for the synthesis of substituted pentalene dimers has not been reported.

One of the most exciting aspects of transition metal chemistry is the formation of new stable metal complexes with unstable organic molecules under normal conditions [17–21]. For example, Pettit *et al.* isolated a stable tricarbonyliron complex by dehalogenation of 3,4-dichlorocyclobut-1-ene with $Fe_2(CO)_9$ [22]. Katz *et al.* have shown that the coordination to metals centres can stabilize pentalene [23–25]. Several organometallic complexes with highly unstable pentalene and its derivatives exhibiting interesting electronic properties have been well investigated [26,27].

On the other hand, alkynyl ligands have been proved to be multifunctional protective ligands for constructing atomically precise metal nanoclusters [28]. Inspired by our previous works [29–31], herein, we were interested in developing copper nanocluster in the presence of $^{c}PrC{\equiv}CH$, $Cu(CF_3COO)_2$ and Cu powder under solvothermal conditions. To our surprise, the reaction underwent multiple *in situ* transformations, resulting in the formation of a pentalene dimer instead of a copper nanocluster. The ensuing pentalene dimer has been comprehensively characterized by

* Corresponding authors.
E-mail addresses: glzhuang@zjut.edu.cn (G. Zhuang), xpw6@sdu.edu.cn (X. Wang), dsun@sdu.edu.cn (D. Sun).
[1] These two authors contributed equally to this work.

https://doi.org/10.1016/j.cclet.2021.10.036
1001-8417/

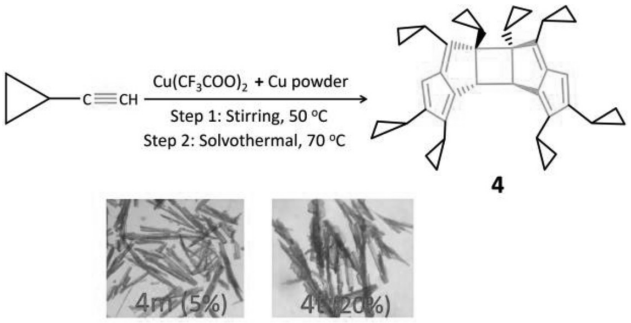

Scheme 1. One-pot synthesis of pentalene dimer derivative.

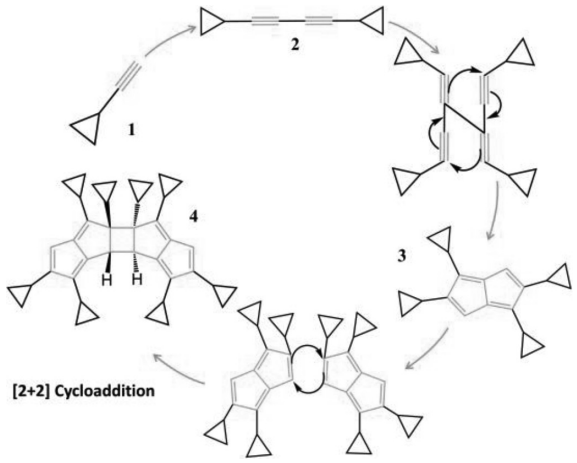

Scheme 2. Proposed transformations and mechanisms for pentalene dimer formation.

NMR, MALDI-TOF/MS, single-crystal X-ray diffraction, UV–vis absorption studies, and further supported by theoretical calculations. To our knowledge, this is the simplest and effective synthetic route for pentalene dimer, and it is also the first example of such compounds characterized by single-crystal X-ray analysis.

The pentalene dimer was synthesized by the reaction of a mixture of $Cu(CF_3COO)_2$, Cu powder and $^{c}PrC{\equiv}CH$ in a 1:4:1 (v/v/v) mixture of DMF-MeOH-MeCN (6 mL). The mixture was reacted at 50 °C by stirring for 6 h, followed by the solvothermal treatment at 70 °C for 36 h (Scheme 1). A large number of orange rod-like crystals (*ca.* 20%) and the small number of yellow rod-like crystals (*ca.* 5%) of $C_{40}H_{44}$ were obtained within two days, which were unambiguously characterized by X-ray crystallography. These compounds have been identified as triclinic (**4t**) and monoclinic (**4m**) polymorphs of $C_{40}H_{44}$. The synthesis details and some basic characterizations are provided in the Supporting information.

Notably, due to the polymorphic nature, only **4t** has been taken as a representative for discussions in detail, but some differences between **4m** and **4t** were also included. The IR spectrum of **4t** exhibits the characteristic stretching vibrations at 3074, 2998, and 1615 cm^{-1}, assigned to =C–H, –C–H and C=C, respectively (Fig. S1 in Supporting information). The ^1H NMR spectrum of **4t** shows the characteristics proton signals for the pentalene (H5) and cyclobutane (H15) at 5.45 and 2.15 ppm as singlet, respectively (Fig. 1a). The chemical shift of methylene (CH_2) and methine proton (CH) on the cyclopropyl ring attached to the cyclobutane ring appear below 0.5 ppm (δ_H –0.33, td; 0.14–0.03, m; 0.19, ddd; 0.50–0.44, m) and 1.47, tt, respectively. Among them, one proton (H13B) on a cyclopropyl ring showing upfield shift (δ_H –0.33), which is caused by the shielding effect from the adjacent pentalene ring. Whereas the protons on the cyclopropyl ring attached to the pentacene core resonated in the region of 0.51–1.83 ppm. Correspondingly, the $^{13}C\{^1H\}$ NMR spectrum shows the characteristics sp^3 tertiary carbon (C15) and sp^3 quaternary carbon (C11) and at 38.26 and 71.53 ppm, respectively (Fig. 1b). The sp^2 tertiary carbons of the pentalene core resonated at 159.66 (C4), 142.90 (C6), 161.99 (C7), 145.47 (C16), 130.53 (C17) ppm, together with sp^2 secondary carbon (C5) at 101.28 ppm. The carbons of the cyclopropyl group appeared in the range of –0.18−15.96 ppm. All these assignments for protons on **4t** were further supported by DEPT135 and 2D NMR spectroscopic data, including ^1H–^{13}C HMBC, ^1H–^1H COSY, and ^1H–^1H NOESY experiments. The detailed data of 1D and 2D NMR are shown in Tables S1, S2 and Figs. S2-S5 (Supporting information). The experimental ^1H and $^{13}C\{^1H\}$ NMR data match well with the theoretical data (Figs. S6-S9 and Table S1 in Supporting information). The composition of **4t** has been further confirmed by the matrix-assisted laser desorption/ionization–time–of–flight (MALDI-TOF) mass spectrum (*m/z* calcd. for $C_{40}H_{44}$ $[M]^+$, 524.343; found 524.391) (Fig. S10 in Supporting information).

High-quality single crystals suitable for X-ray diffraction of pentalene dimers were grown by slow evaporation of the reaction mixture for 2–3 days. It crystallizes as a polymorph in the centrosymmetric triclinic and monoclinic crystal system with the space group of *P*-1 and $P2_1/c$, respectively (Table S3 in Supporting information). Although some reports on pentalene dimers are well documented, and various geometries and isomers were suggested, no crystal structures with such kinds of dimers were reported to date. To our knowledge, this is the first example of a pentalene dimer, which has been unambiguously determined by single-crystal X-ray analysis. Due to the similarity of their molecular structures, we take the triclinic system (**4t**) as a representative for discussions in detail below.

The **4t** exhibits a stair-like structure (Fig. 2) with two pentalene units fused on a central cyclobutane ring left and right. The formula of **4t** is $C_{40}H_{44}$. Of note, a total of eight cyclopropyl groups attached to above dimerized pentalene core, with six on the pentalene and the other two on the central cyclobutane ring. The bond length of the four-membered cyclobutane ring is slightly longer than those of carbon-carbon single bonds and varies in the range of 1.56−1.60 Å. The dimerized pentalene core showed C_{2h} symmetry, alternate long (1.449(2), 1.4905(19), 1.5337(2) and 1.491(2) Å for C5–C6, C4–C17, C7–C11, and C15–C16, respectively) and short bonds (1.359(2), 1.354(2), and 1.353(2) Å for C4–C5, C6–C7 and C16–C17, respectively), which are in good agreement with the previously reported structures of pentalene derivatives (Fig. 2a, Table S4 in Supporting information) [32]. The cyclopropyl C–C bond lengths vary in the range of 1.473(3)−1.515(2) Å, indicating the single bond nature. The conjugated pentalene ring (A) deviates from the nonconjugated ring (B) with an average of 2.62° and 2.56° for **4t** and **4m**, respectively (Figs. S11 and S12 in Supporting informaion). The dihedral angles between the planes of the two pentalene units are 11.55° and 10.48° for **4t** and **4m**, respectively (Figs. S13 and S14 in Supporting information). The bond lengths and bond angles in both polymorphs are similar. More interestingly, through C–H$\cdots\pi$ and van der Waals interactions, $C_{40}H_{44}$ molecules in **4t** and **4m** packed in *ABAB* and *ABCD* fashions along a and c axis, respectively, (Figs. S15 and S16 in Supporting information), which dictate their different crystallized space groups in solid-state. The bond lengths comparison between the crystal structure and geometrically optimized structure (*vide infra*) is in good agreement, as shown in Fig. S17 (Supporting information).

To shed insights into the reaction mechanism of the pentalene dimer, a process of dimerization, cyclization followed by cycloaddition is proposed. The mechanism for the formation of **4** is illustrated in Scheme 2. The proposed mechanism can be roughly divided into two steps. The first step is the Giles Gasser dimer-

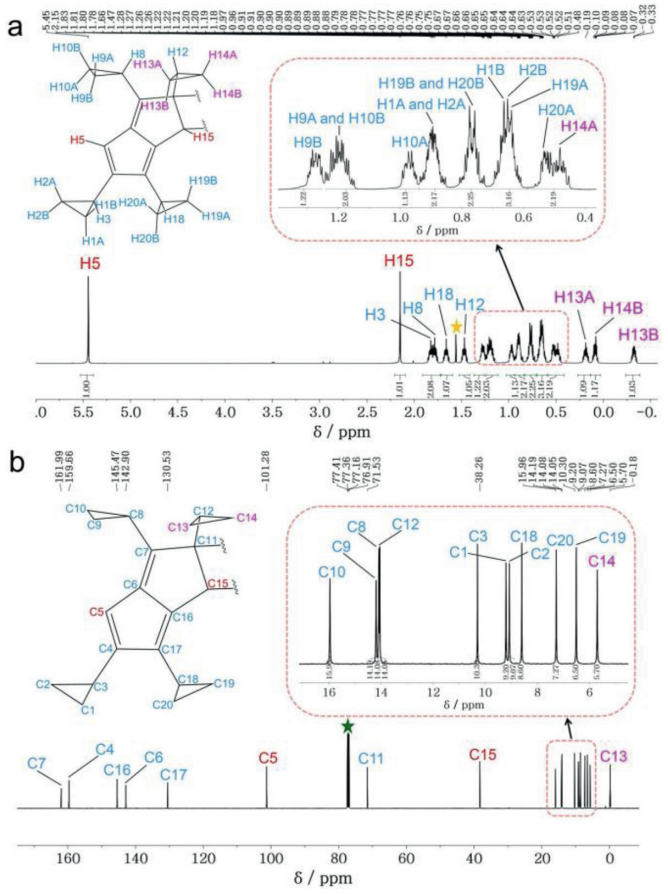

Fig. 1. (a) ^{1}H NMR and (b) $^{13}C\{^{1}H\}$ NMR spectrum of **4t** in $CDCl_3$. The asterisks indicate the resonance of the residual solvent signals.

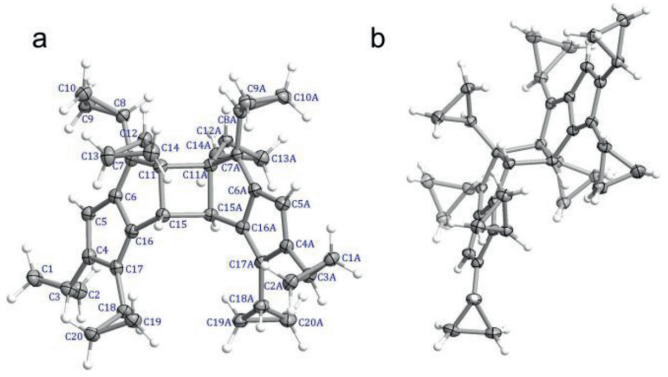

Fig. 2. Crystal structure of pentalene dimer (a) front view (b) side view. Thermal ellipsoids are shown at the 50% probability level.

ization of terminal aliphatic alkyne (**1**) in the presence of Cu(I) *in situ* generated and oxygen as an oxidant to produce (**2**). The second step is the cyclotetramerization of a dimerized alkyne to give pentalene (**3**), which is prone to dimerization in order to relieve its electronic strain resulting from the conjugated 8π antiaromatic system to yield pentalene dimer (**4**) finally. Bailey *et al.* isolated and structurally characterized stable dihydropentalenes (Ph_4PnH_2) from cyclotetramerization of phenylacetylene catalyzed by $PdCl_2$, where there is no driving force for dimerization in the fulvenic 6π aromatic dihydropentalene [33].

Following the above similar synthetic route, we also performed a series of parallel reactions in the presence of only $Cu(CF_3COO)_2$, only copper powder, or in the absence of $Cu(CF_3COO)_2$ and copper powder. All these reactions do not produce the pentalene dimer, confirming that both $Cu(CF_3COO)_2$ and Cu powder are essential for the reaction. Furthermore, to understand the influence of substituents on the terminal alkyne, the reactions of phenyl and *tert*–butyl substituted alkyne, *i.e.*, phenyl acetylene and *tert*–butyl acetylene were carried out under identical conditions. Both the reactions yielded some uncharacterized products. This may be due to the fact that the steric hindrance of the phenyl substituent is greater than the cyclopropyl group and does not engage in oxidative coupling. On the other hand, electron-donating tendency imposed by the *tert*–butyl substituent of *tert*–butyl acetylene is not enough to induce the oxidative coupling.

Although we did not obtain single crystals of Cu(I) complexes, Cu(I) species in mother liquor catalyzed the formation of pentalene dimer. In order to confirm the presence of Cu(I) species in mother liquor, we performed the ESI-MS of the mother liquor. As depicted in Fig. S18 (Supporting information), we observe three peaks centered at *m/z* 576.8051 (**1a**), 706.7958 (**1b**) and 834.7783 (**1c**). After carefully checking the separation between the isotopes, we found that **1a**-**1c** are monovalent species and are assigned to $[Cu_5(^cPrC{\equiv}C)_4]^+$ (**1a**, calcd. *m/z* 576.8022), $[Cu_6(^cPrC{\equiv}C)_5]^+$ (**1b**, calcd. *m/z* 706.7693) and $[Cu_7(^cPrC{\equiv}C)_6]^+$ (**1c**, calcd. *m/z* 834.7381), respectively (Table S5 in Supporting information).

To further identify the pentalene dimer formation mechanism, spin-polarized density functional theory calculations were performed at the theoretical level of D3(BJ)-B3LYP/6-31+G(d,p)//M06/TZVP by using Gaussian 09 package [34]. Four possible reaction pathways were considered: Path 1 (Fig. 3) and Paths 2–4 (Fig. S19), for details see Figs. S19-S70 and Tables S6-S56 (Supporting information). In the initial reaction, the cyclopropyl alkyne attacks on the Cu to form **Int1–2** with the releasing energy of 2.84 kcal/mol, indicating that the triple bond of cyclopropyl alkyne is thermodynamically activated. Then, the **Int1–2** undergoes subsequent reactions in two ways: (1) removing the H of C–H to form **Int1–3** (Path 1); (2) bonding with a cyclopropyl alkyne to become **Int3–1** (Path 3), respectively. As shown in Fig. 3 and Fig. S19a, the **Int1–3** is formed by removing the H atom of C–H from **Int1–2** with the required energy of 33.84 kcal/mol. After removing the H, the C of **Int1–3** with one unpaired electron is beneficial to react with the next cyclopropyl alkyne to produce **Int1–4**. In the uphill process with the activation energy of 17.29 kcal/mol (**TS1–2**), the C–C coupling occurs from **Int1–4** to **Int1–5**. Meanwhile, **Int1–5** has two reaction ways: (1) directly bond with another **Int1–5** intermediate (Path 1), (2) combine with the reactant cyclopropyl alkyne for subsequent reactions (Path 2). For the former (Fig. 3), both carbon atoms in **Int1–5** connected to Cu gradually get closer to generate **Int1–7** *via* intermediate **Int1–6** and **TS1–3**. Both carbon atoms feature doublets state, resulting in the activation energy of 21.92 kcal/mol in this reaction process and the reducing energy of 11.18 kcal/mol compared to **Int1–1**, thermodynamically. The pentalene (**Int1–9**) was gained from the intermediate of **Int1–7** and **Int1–8** through two-step successive C–C coupling of **TS1–4** (5.32 kcal/mol) and **TS1–5** (32.84 kcal/mol), respectively. Such reaction features an exothermic process with about 106.17 kcal/mol for **Int1–1**.

Pentalene (**Int1–9**) is synthesized from the cyclopropyl acetylene through the above four reaction paths. Furthermore, **Int1–9** bonds with the intermediate after removing Cu from **Int1–9** to form **Int1–10** with larger exothermic energy of 226.39 kcal/mol. The best way to form pentalene dimer from **Int1–10** is taken into account. **Int1–10** directly crosses the 38.63 kcal/mol energy barrier to produce the final product. In general, the synthesis of pentalene dimer is mainly through multistep carbon-carbon coupling from the cyclopropyl alkyne. In view of the activation energy barriers, among the four paths, Path 1 with the rate-determining step of 38.63 kcal/mol is thermodynamically preferable.

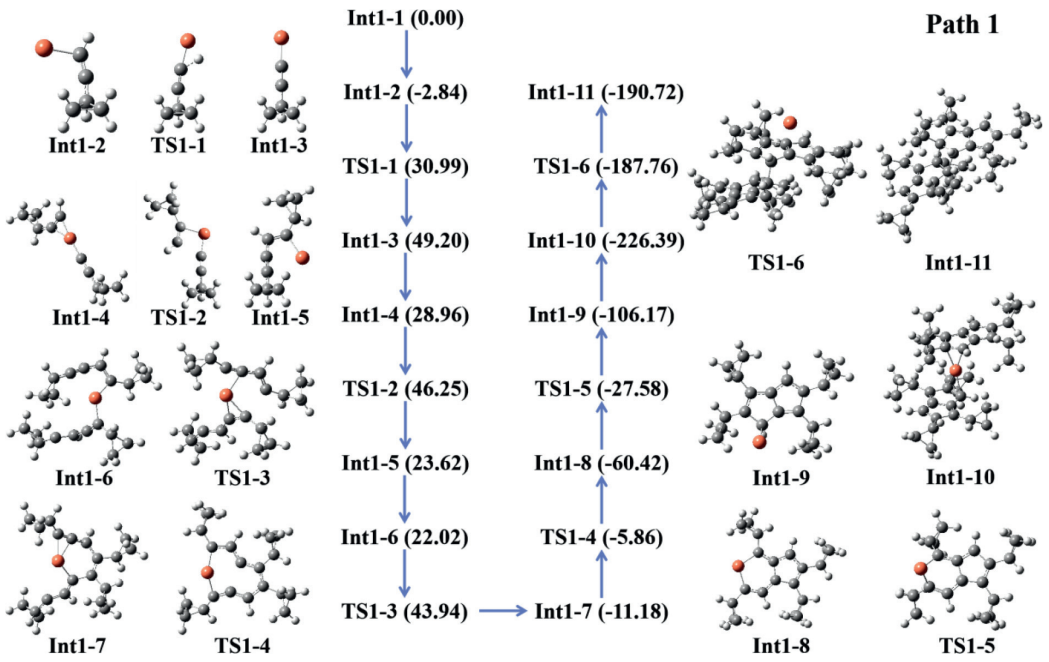

Fig. 3. Gibbs free energy diagram of reaction coordinates (Path 1) for the product pentalene dimer formation from the reactant cyclopropyl alkyne at 298.15 K, unit: kcal/mol.

The electronic absorption spectrum of **4t** was recorded in dichloromethane (DCM) (Fig. S71 in Supporting information). The absorption band at 391 nm may be assigned to the π-π^*, whereas the shoulder band and intense band at 326 and 298 nm, respectively, are credited to the n-π^* transitions. Furthermore, to get a deep insight into the electronic transitions, solid-state UV–vis spectrum under reflectance mode was measured (Fig. S72a in Supporting information). The bandgap energy (E_g) for **4t** and **4m** was calculated to be 2.18 and 2.2 eV, respectively (Fig. S72b in Supporting information). The slightly different bandgaps of two polymorphs of $C_{40}H_{44}$ should rise from the different molecule packing in bulk phases.

To understand the electronic structure and the origin of the absorption band of **4t**, density functional theory (DFT) and time-dependent density functional theory (TD-DFT) calculations were carried out employing Gaussian 09 program (Revision A.02) 6–31G(d,p) basis set for C, and H at B3LYP (Becke-3-Lee-Yang-Parr) level (details see Supporting information). The solvent calculation was conducted in DCM using the polarized continuum model (PCM). The frontier molecular orbital (FMO) plots of the **4t** are shown in Fig. S73 (Supporting information). The HOMO of **4t** is delocalized over the pentalene subunits, and the LUMO is delocalized over the pentalene unit attached to the cyclobutane ring. The calculated UV–vis absorption spectrum of **4t** was simulated using TD-DFT energy (vertical excitation and oscillator strengths) calculations on the optimized ground-state structures (Tables S57 and S58 in Supporting information), and these data are in good correlations with the experimental absorption spectrum (Fig. 4). The theoretical bandgap energies of **4t** calculated at B3LYP level equal to 3.56 eV and matches the respective optical band energy of 3.12 eV (in DCM). The TD-DFT calculation shows that the main absorption band at ~426 nm is contributed by the transitions from HOMO to LUMO, whereas the band at 298 nm is contributed by the transitions from HOMO-2 and HOMO-3 to LUMO. The absorption band centered at 258 nm is originated from the transitions from HOMO-2 to LUMO and LUMO+1 (Fig. 5).

In conclusion, a simple and efficient route to synthesize a novel cyclopropyl substituted pentalene dimer has been serendipitously discovered and successfully characterized by X-ray crystallography, demonstrating the first example of such compounds in the solid-state. The reaction starting from ^{c}PrC≡CH has undergone multiple transformations, including acetylenic coupling, followed by cyclization and [2 + 2] cycloaddition, and finally pentalene dimer is obtained. The reaction mechanism was further investigated and elucidated in detail by theoretical calculations. The rate-determining step with the activation energy of 38.63 kcal/mol clearly indicated that Path 1 was the most thermodynamically preferred among the four proposed paths. The successful synthesis of pentalene dimer

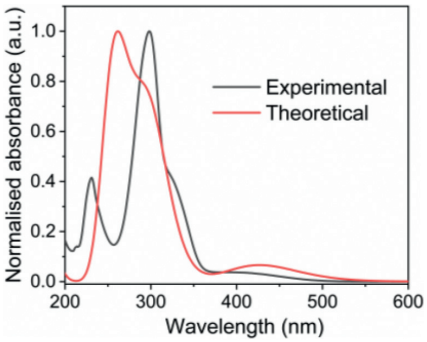

Fig. 4. Comparison of experimental and computed (6-31G(d,p) level by B3LYP methods) absorption spectra of **4t**.

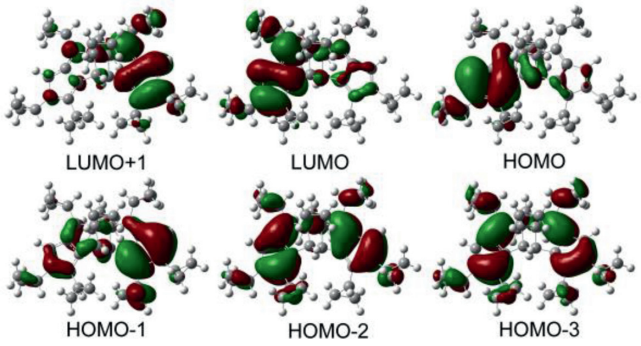

Fig. 5. Frontier molecular orbitals of **4t** at the B3LYP/6-31G(d,p) level in DCM solvent using PCM model.

avoids the pyrolysis, flammable organolithium or Grignard reagents and is performed utilizing readily available components under ambient conditions. We believe that the proposed synthetic route would provide new insights into the synthesis and investigation of the physicochemical properties of the elusive pentalene derivatives.

Declaration of competing interest

The authors declare no conflict of interest.

Acknowledgments

This work was financially supported by the National Natural Science Foundation of China (Nos. 91961105, 21822107, 21571115, 21827801), the Natural Science Foundation of Shandong Province (Nos. ZR2019ZD45, JQ201803 and ZR2017MB061), and the Taishan Scholar Project of Shandong Province of China (Nos. tsqn201812003 and ts20190908). Project for Scientific Research Innovation Team of Young Scholar in Colleges and Universities of Shandong Province (No. 2019KJC028), Natural Science Foundation of Shandong Province (No. ZR2020ZD35). We thank Y. Z. Tan (Xiamen University), Y. Wang, Z. H. Xu, and L. Liu (Shandong University) for helpful discussions.

Supplementary materials

Supplementary material associated with this article can be found, in the online version, at doi:10.1016/j.cclet.2021.10.036.

References

[1] H.J. Lindner, et al., Pentalene und dihydropentalene, in: T. Asao, G. Becker, H. Blaschke, et al. (Eds.), Carbocyclic π-Electron Systems, 4th Ed., Georg Thieme Verlag, Stuttgart, 1985, pp. 103–122.
[2] H.S. Xin, B. Hou, X.K. Gao, Acc. Chem. Res. 54 (2021) 1737–1753.
[3] H. Hopf, Angew. Chem. Int. Ed. 52 (2013) 12224–12226.
[4] H. Hou, X.J. Zhao, C. Tang, et al., Nat. Commun. 11 (2020) 3976.
[5] B. Liu, F. Yu, M. Tu, et al., Angew. Chem. Int. Ed. 58 (2019) 3748–3753.
[6] Z.E. Zhang, Y.Y. An, B. Zheng, et al., Sci. China Chem. 64 (2021) 1177–1183.
[7] Zerubba U. Levi, T.Don Tilley, J. Am. Chem. Soc. 131 (2009) 2796–2797.
[8] H. Oshima, A. Fukazawa, S. Yamaguchi, Angew. Chem. Int. Ed. 56 (2017) 3270–3274.
[9] M. Saito, Symmetry 2 (2010) 950–969.
[10] J. Zhao, K. Oniwa, N. Asao, et al., J. Am. Chem. Soc. 135 (2013) 10222–10225.
[11] S. You, M. Neuenschwander, Chimia 50 (1996) 24–26.
[12] S. You, S. Chai, N. Schwarz, et al., Helv. Chim. Acta 80 (1997) 1627–1638.
[13] H. Meier, A. Pauli, P. Kochhan, Synthesis (1987) 573–574.
[14] H. Meier, A. Pauli, H. Kolshorn, et al., Chem. Ber. 120 (1987) 1607–1610.
[15] M.S. Baird, C.B. Reese, Tetrahedron Lett. 33 (1976) 2895–2898.
[16] I. Fleischhauer, U.H. Brinker, Chem. Ber. Recl. 120 (1987) 501–506.
[17] S.A.R. Knox, F.G.A. Stone, Acc. Chem. Res. 7 (1974) 321–328.
[18] C. Papatriantafyllopoulou, E.E. Moushi, A.J. Tasiopoulos, Chem. Soc. Rev. 45 (2016) 1597–1628.
[19] M. Manoli, S. Alexandrou, A.J. Tasiopoulos, Angew. Chem. Int. Ed. 55 (2016) 679–684.
[20] G. Feng, M. Zhang, P. Wang, et al., PANS 116 (2019) 17654–17658.
[21] F.K.W. Kong, M.C. Tang, Y.C. Wong, et al., J. Am. Chem. Soc. 139 (2017) 6351–6362.
[22] L. Watts, J.D. Fitzpatrick, R. Pettit, J. Amer, Chem. Soc. 87 (1965) 3253–3254.
[23] T.J. Katz, M. Rosenberg, J. Am. Chem. Soc. 85 (1963) 2030–2031.
[24] T.J. Katz, N. Acton, J. McGinnis, J. Am. Chem. Soc. 94 (1972) 6205–6206.
[25] T.J. Katz, N. Acton, J. Am. Chem. Soc. 94 (1972) 3281–3283.
[26] O.T. Summerscales, F.G.N. Cloke, Coord. Chem. Rev. 250 (2006) 1122–1140.
[27] S.M. Boyt, N.A. Jenek, U. Hintermair, Dalton Trans. 48 (2019) 5107–5124.
[28] Z. Lei, X.K. Wan, S.F. Yuan, et al., Acc. Chem. Res. 51 (2018) 2465–2474.
[29] B.L. Han, Z. Liu, L. Feng, et al., J. Am. Chem. Soc. 142 (2020) 5834–5841.
[30] H.Y. Zhuo, H.F. Su, Z.Z. Cao, et al., Chem. Eur. J. 22 (2016) 17619–17626.
[31] H.Y. Zhuo, A.Y. Hu, L. Feng, et al., J. Clust. Sci. 29 (2018) 1017–1022.
[32] X. Yin, Y. Li, Y. Zhu, et al., Org. Lett. 13 (2011) 1520–1523.
[33] P.M. Bailey, B.E. Mann, I.D. Brown, et al., Chem. Commun. (1976) 238–239.
[34] M.J. Frisch, G.W. Trucks, H.B. Schlegel, et al., Gaussian 09, Revision C, 01, Gaussian, Inc., Wallingford, CT, USA, 2009.